FEMS Microbiology Ecology, 2024, 100, fiae122
DOI: 10.1093/femsec/fiae122
Advance access publication date: 11 September 2024
Research Article

Deciphering root-associated microbial communities in asymptomatic oil palm seedlings exposed to *Ganoderma boninense*: new insight into disease tolerance of oil palms

Lisim Ho [1,*], Chengyu Lai[2], Leona D.J. Daim[1], Normahnani M. Noh[1], Yunci Yap[1], Julia Ibrahim[1], Cheekeng Teh[1]

[1]SD Guthrie Technology Centre Sdn Bhd, 1st Floor Block B, UPM-MTDC Technology Centre III, Serdang, 43400, Selangor, Malaysia
[2]Inong Agriculture Co., Ltd., 3F, 48 Fuxing North Road Zhongshan district, Taipei, 104102, Republic of China
*Corresponding author. SD Guthrie Technology Centre Sdn Bhd, 1st Floor Block B, UPM-MTDC Technology Centre III, Serdang, 43400, Selangor, Malaysia.
E-mail: ho.li.sim@sdguthrie.com
Editor: [Angela Sessitsch]

Abstract

Understanding the microbial communities in asymptomatic oil palm seedlings is crucial for developing disease-suppressive microbiota against basal stem rot (BSR) in oil palm. In this study, we compared the microbial communities in bulk soil, rhizosphere, and endosphere of control, asymptomatic, and symptomatic seedlings following inoculation with *Ganoderma boninense*. Our findings revealed significant shifts in microbial structure and interactions, particularly in asymptomatic seedlings. Both Actinobacteriota and Ascomycota were notably enriched in these samples, with Actinobacteriota identified as keystone taxa. Long-read shotgun metagenomics demonstrated that 67.4% of enriched Actinobacteriota taxa were unique to asymptomatic seedlings. Similarly, Ascomycota members showed significant enrichment, suggesting their potential role in BSR suppression. The consistent identification of these phyla across various analyses underscores their importance in disease resistance. This is the first report detailing the shifts in prokaryotic and fungal communities in asymptomatic and symptomatic seedlings, offering insights into potential disease-suppressive taxa across three compartments: bulk soil, rhizosphere, and endosphere of oil palm seedlings.

Keywords: basal stem rot disease; disease suppression; *Ganoderma boninense*; oil palm disease; plant–pathogens interactions; root microbiome

Introduction

Oil palm (*Elaeis guineensis*, Jacq.) is the most efficient oil crop in the world, capable of producing eight times more oil per hectare than other oil crops (Nomanbhay et al. 2017). Oil palm is cultivated near equator in West Africa, South America, Southeast Asia, Papua New Guinea (PNG), and Solomon Islands (SI). Several factors are critical to oil palm productivity, including pests and disease, selective breeding of planting material, agronomic practices (planting density, canopy management, pollination, and harvesting), rainfalls, nutrients, and soil type. Suboptimal conditions can slash productivity by >70%. In severely disease-infested areas, productivity can nearly eliminate yields (Woittiez et al. 2017).

Oil palm diseases vary by region. In West Africa (Turner 1981, Flood 2006, Gorea et al. 2020), vascular wilt disease caused by *Fusarium oxysporum* F. sp. *elaeidis* is a significant threat, while in South America, bud rot, or spear rot, caused by *Phytophthora palmivora*, is a major concern. In Southeast Asia and Oceania, basal stem rot (BSR) caused by *Ganoderma boninense* is the most devastating (Pilotti et al. 2002, Rees et al. 2007, Gorea et al. 2020). Initially affecting older palms, BSR now also impacts younger ones, especially in replanted areas. Severe infections can occur within 2 years after replanting, particularly when old palm stumps are left in the ground (Subagio and Foster 2003), leading to a buildup of pathogens (Turner 1981, Gorea et al. 2020). Infections typically result in death within 6–12 months for young palms and 2–3 years for mature ones (Jackson 2017).

Extensive research has addressed BSR (Goh et al. 2020, Husin et al. 2020, Khaled et al. 2020), from disease management (Maluin et al. 2019, Chong et al. 2020, Goh et al. 2020), early identification (Ahmadi et al. 2017, Khosrokhani et al. 2018, Khaled et al. 2020, Kresnawaty et al. 2020), plant and disease biology (Durand-Gasselin et al. 2005, Rees et al. 2009, Chong et al. 2017, Wong et al. 2019, Sulaiman et al. 2020), to monitoring (Ibrahim et al. 2020) and soil microbial ecology (Amran et al. 2016, Virdiana et al. 2019, Lo and Chong 2020). Integrated pest management (IPM) is widely embraced as a control method, encompassing agronomic, biological, and chemical treatments. While these measures effectively delay disease progression and extend oil palm lifespan, the persistent prevalence of BSR indicates a need for deeper understanding and more effective control strategies. A proactive, promising long-term solution involves breeding for *Ganoderma*-tolerant planting materials. A large-scale screening is ongoing to identify tolerant progenies for breeding purposes. The industry practices involve artificially inoculating germinated seeds or 3-month-old seedlings with the pathogen and monitoring disease progression over time (Turnbull et al. 2014). SD Guthrie utilizes a similar approach on 6-month-old seedlings to ensure a better reflectiveness of the tolerance in the field. Host genetics play a crucial role in disease tolerance, and studying the underground microbial communities

Received 2 August 2024; **revised** 5 September 2024; **accepted** 11 September 2024

associated with asymptomatic seedlings can reveal potential disease-suppressing microbes. Typically, one-dimensional studies that focus solely on the host's genetic potential are limited to specific environments, which partly explains the poor correlation of tolerance between nursery and field conditions (Mendes et al. 2011, Jochum et al. 2019, Jones et al. 2019). Consequently, researchers have ventured into studying underground microbial communities. While previous studies have compared microbial communities between healthy and diseased hosts (Iasmartua 2018), or between asymptomatic and symptomatic samples (Anothai and Chairin 2022), we questioned whether secondary infections in symptomatic samples might alter microbial characteristics and distort observations.

In our research, we utilized host materials with a narrow genetic background, allowing a more precise identification of microbial compositions crucial for disease suppression, minimizing genetic variability. Our novel approach compares asymptomatic hosts with control, which were healthy, unexposed hosts, aiming to accurately identify disease-suppressive microbial traits. We hypothesized that the presence of pathogen-suppressive microbes in the root zone is associated with asymptomatic seedlings.

This study aims to: (i) analyze the structure, function, and interactions of belowground microbial communities in response to pathogen inoculation in two distinct host responses (asymptomatic and symptomatic) versus control, and (ii) identify microbial taxa potentially involved in suppressing BSR. We employed 16S rRNA and ITS gene amplicon sequencing to profile prokaryotic and fungal communities, supplemented by Nanopore shotgun metagenomics sequencing in a subset of samples. We compared microbial communities in soil, rhizosphere, and endosphere between control and asymptomatic seedlings, using symptomatic seedlings as a baseline.

Materials and methods

Planting material, treatment preparation, trial description, sample selection, and sample processing

Oil palm germinated seeds (*dura* × *pisifera*) were provided by the Oil Palm Breeding Unit, SD Guthrie Research Sdn Bhd. All preparations for the nursery trial were carried out according to the Oil Palm Nursery Technique Good Agricultural Practices (SD Guthrie). Seedlings were maintained under artificial shade with 50% light cutoff. For both control and inoculated seedlings, the experiment was replicated in four plots, each containing 16 seedlings, totaling 64 seedlings ($n = 64$). The trial was conducted using a randomized complete block design (RCBD).

For fungal inoculum preparation, the *G. boninense* strain PER71 was obtained from the Malaysian Palm Oil Board (MPOB). The fungus was cultured and maintained on potato dextrose agar (PDA). Rubber wood blocks (RWB) were custom cut to 6 × 6 × 6 cm. All RWB were sterilized in an oven at 80°C overnight before autoclaving at 121°C for 1 h. Each RWB was placed in a plastic bag filled with 120 ml of malt extract (ME) agar. These bags were sealed, autoclaved at 121°C for 15 min, and left to solidify overnight. The 7-day-old *G. boninense* culture from a PDA plate was divided into four parts, and two parts were inoculated on the sterilized RWB. The inoculated RWB were incubated at 25–28°C for ∼150 days until the mycelia completely covered the RWB.

Germinated seeds were sown in 10″ × 12″ polybags containing topsoil and sand in a 2:1 ratio. The seedlings were transplanted into 15″ × 18″ polybags when they were 6 months old, along with artificial inoculation using *Ganoderma*-inoculated RWB. During transplanting, fully colonized RWB were placed in the middle of the bag, and the seedlings were placed in close contact with the RWB using a sitting technique. The 6-month-old control and inoculated seedlings were monitored until they were 18 months old (48 weeks post-inoculation). Disease progression was assessed based on the Disease Severity Index (DSI), for the bole, as described by Normahnani (2016). Ten seedlings that remained as class 0 DSI at (no internal rot observed at bole) week 48 post-inoculation were selected as asymptomatic samples, while 10 seedlings exhibiting class 4 DSI (>90% rotting of tissues observed at bole) were selected as symptomatic samples. In addition to asymptomatic and symptomatic seedlings, 10 control seedlings were also selected (Fig. 1).

DNA extraction, PCR amplification, amplicon sequencing (Illumina), data processing, and data analysis

For each sample, total DNA was extracted from 0.5 g of soil using the DNeasy Powersoil Kit (Qiagen, Germany) according to the manufacturer's instructions. The concentration and quality of genomic DNA were measured using a NanoDrop ND-2000 spectrophotometer (NanoDrop Technologies, Wilmington, DE, USA). Two primer sets were used for whole community amplicon sequencing for both prokaryotic and fungal communities. The primer pair ITS3 (5′-GCATCGATGAAGAACGCAGC-3′)/ITS4 (5′-TCCTCCGCTTATTGATATGC-3′) (White 1990) was used for fungal community amplification, while the primer pair 515F (5′-GTGYCAGCMGCCGCGGTAA-3′)/926R (5′-CCGYCAATTYMTTTRAGTTT-3′) (Parada et al. 2016) was used for the V4–V5 hypervariable regions of the prokaryotic 16S rRNA gene.

The primer pairs were modified for sequencing by adding the forward Illumina Nextera adapter, a two-base-pair "linker" sequence, and a unique 7-bp barcode sequence at the 5′ end of the forward primer, and the appropriate reverse Illumina Nextera adapter and linker sequence at the 5′ end of the reverse primer. Briefly, 27 cycles were performed to amplify fungal templates and 25 cycles to amplify prokaryotic templates. The PCR products were then purified using a PCR Purification Kit (Axygen Bio, USA) and pooled in equimolar concentrations of 10 ng/mL before sequencing. Finally, paired-end sequencing of fungal and prokaryotic amplicons was carried out on the Illumina MiSeq sequencer.

The bulk soil and rhizosphere soil, along with roots of these seedlings, were subjected to whole microbial community DNA extraction. Five samples from each treatment and control group with good DNA yield and quality were subjected to 16S rRNA and ITS gene amplicon sequencing for prokaryotic and fungal community profiling.

For data processing, sequence adaptors and low-quality reads were removed from paired end reads using BBDuk of the BBTools package (https://sourceforge.net/projects/bbmap/). Following this, the forward and reverse reads were merged using USEARCH v11.0.0667 (https://www.drive5.com/usearch/). Sequences shorter than 150 bp or longer than 600 bp were removed before alignment against the SILVA database (Release 132) for 16S rRNA gene or the UNITE ITS database for the fungal ITS region. VSEARCH v2.6.2 was used to inspect for chimeric errors. Upon completion of quality assessments, reads were subjected to de novo clustering into OTUs (operational taxonomic units) at 97% similarity using UPARSE v11.0.667, with spurious doubletons removed from downstream processing. A single representative sequence was randomly chosen from each OTU, and Pynast (https://www.ncbi.nlm.nih.gov/pubmed/19914921) was used to align and construct a phylogenetic tree against the SILVA 132 16S rRNA gene

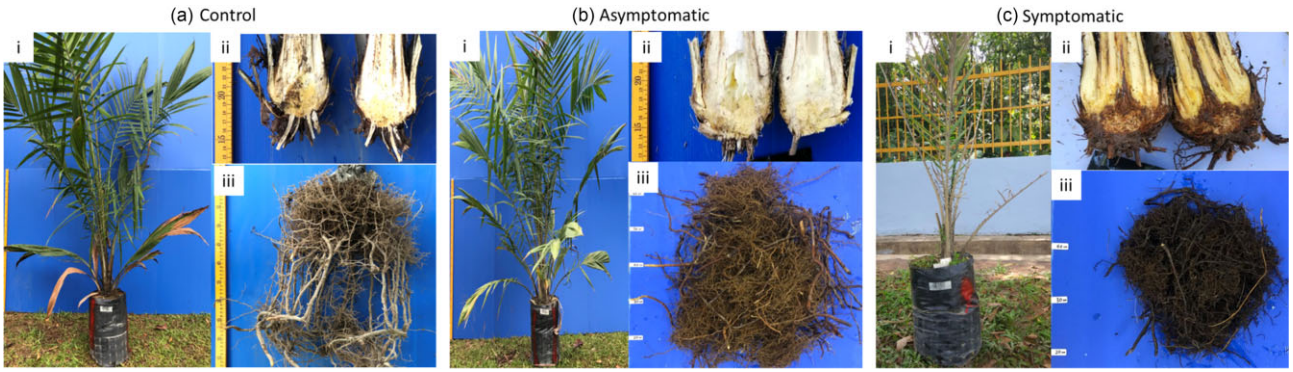

Figure 1. Oil palm seedlings inoculated with *G. boninense* strain PER71 (a) control; (b) asymptomatic; and (c) symptomatic; (i) whole seedlings; (ii) asymmetry dissection of seedling bole; and (iii) root mass of seedlings.

database, while taxonomic assignment of OTUs was done using QIIME V1.9.1 against the SILVA 16S rRNA gene database (release 132).

Microbial diversity was estimated using Chao 1 richness and Shannon indices. Variation in microbial composition among samples of different treatments was analyzed. Bray-Curtis dissimilarity was computed and PCoA (Principal Coordinate Analysis) was performed to visualize the variation in community composition. Multivariate non-parametric analysis, including PERMANOVA (Permutational Multivariate Analysis of Variance), was carried out to test the significance of differences between samples. Differential abundance analysis was conducted using DESeq2, a method employing shrinkage estimation for dispersions and fold changes with improved stability and interpretability of estimates, enabling a quantitative analysis focused on both the strength and detection of differential abundance. Hierarchical clustering heatmaps were constructed to provide insight into the relative abundance, phylogenetic relatedness, and similarity between samples. LEfSe, linear discriminant analysis (LDA) effect size, was performed to identify potential taxa associated with symptomatic and asymptomatic samples.

All statistical analyses were done in R package V3.6.1 using the following packages: vegan, Phyloseq, Microbiome, Microbiomeutilities, metacoder, and Tax4Fun2.

Shotgun metagenomics sequencing (nanopore technology) and data processing

DNA from rhizosphere samples, one each from control, asymptomatic, and symptomatic groups, was subjected to shotgun metagenomics sequencing. Library preparation of extracted genomic DNA was performed using the Oxford Nanopore Technologies (ONT) Ligation Sequencing Kit according to the manufacturer's protocol. Libraries were sequenced on the ONT PromethION platform using R9.4.1 flow cells.

For sequence assembly, the adapters in the reads were removed using Porechop v0.2.4 (GitHub—rrwick/Porechop: adapter trimmer for Oxford Nanopore reads). High-quality reads (Phred score > Q7) were selected using LongQC v1.2.0b (GitHub—yfukasawa/LongQC: longQC is a tool for the data quality control of the PacBio and ONT long reads). Reads shorter than 1 K bps were filtered using Filtlong v0.2.0 (GitHub—rrwick/Filtlong: quality filtering tool for long reads) and assembled into Metagenome-Assembled Genomes (MAGs) using Flye v2.8.3 (GitHub—fenderglass/Flye: de novo assembler for single-molecule sequencing reads using repeat graphs). The MAGs were polished twice with Racon v1.4.21 (GitHub—isovic/racon: ultrafast consensus module for raw de novo genome assembly of long uncorrected reads). Note: This was the original repository, which will no longer be officially maintained. Please use the new official repository here. Remaining systematic errors were then removed by Medaka v1.2.5 (GitHub—nanoporetech/medaka: sequence correction provided by ONT research) and Homopolish v0.0.2 (GitHub—ythuang0522/homopolish: high-quality nanopore-only genome polisher).

For taxonomic classification and quantification, the quality-controlled reads were aligned against the NCBI RefSeq database using minimap2 and mash dist (GitHub—marbl/Mash: fast genome and metagenome distance estimation using MinHash) to select candidate references and classified to taxon using Average Nucleotide Identity (ANI). The microbial proportion was calculated by read count and corrected by each genome size of the species.

For CDS (coding sequence) annotation, the CDS and structural RNAs were annotated using DFAST v1.2.15 with parameters for metagenomes (GitHub—nigyta/dfast_core: DDBJ Fast Annotation and Submission Tool). KEGG annotations were assigned by searching against KOfam, a customized HMM database of KEGG orthologs (KOs), using KofamScan v1.3.0 (https://github.com/takaram/kofam_scan).

Network analysis

For network analysis, a microbial co-abundance network was constructed using NAMAP with the Spearman's rank correlation algorithm via MetagenoNets to elucidate the ecological interactions among the microbiota in the roots of oil palm. Features were filtered using a prevalence cut-off of 0.0005, occurrence in a minimum of 10% of samples, with a significance cut-off of $\alpha = 0.05$, 250 bootstrap iterations, and a correlation cut-off at critical R. Identification of putative keystone taxa was performed using the Cytohubba plugin (Chin et al. 2014), where the putative keystone taxa were estimated primarily based on the Maximal Clique Centrality (MCC) index, validated with multiple indices including degree, edge percolated component (EPC), maximum neighbourhood component (MNC), density of maximum neighbourhood component (DMNC), and the six centralities (bottleneck, eccentricity, closeness, radiality, betweenness, and stress).

Statistical analysis

The disease incidence and severity, abundances of taxa, and alpha diversity indices between control, symptomatic, and

Table 1. Total read count, richness (Chao 1), and Shannon diversity indices of prokaryotes and fungi for control, asymptomatic and symptomatic samples in the bulk soil, rhizosphere soil, and endosphere samples.

			Total read count		Chao1		Shannon index	
Domain	Niches	Treatment	Asymp	Symp	Asymp	Symp	Asymp	Symp
Prokaryotes	Soil	Ctrl	*					
		Asymp						
	Rhizosphere	Ctrl						
		Asymp				*		*
	Endosphere	Ctrl		*	*	*		*
		Asymp		*		*		*
Fungi	Soil	Ctrl						
		Asymp						
	Rhizosphere	Ctrl						
		Asymp						
	Endosphere	Control	*				*	
		Asymp				*		

*Indicates significant difference comparing the pair at 95% confidence interval (Student's *t*-test), $n = 5$; Ctrl = Control, Asymp = Asymptomatic, and Symp = Symptomatic.

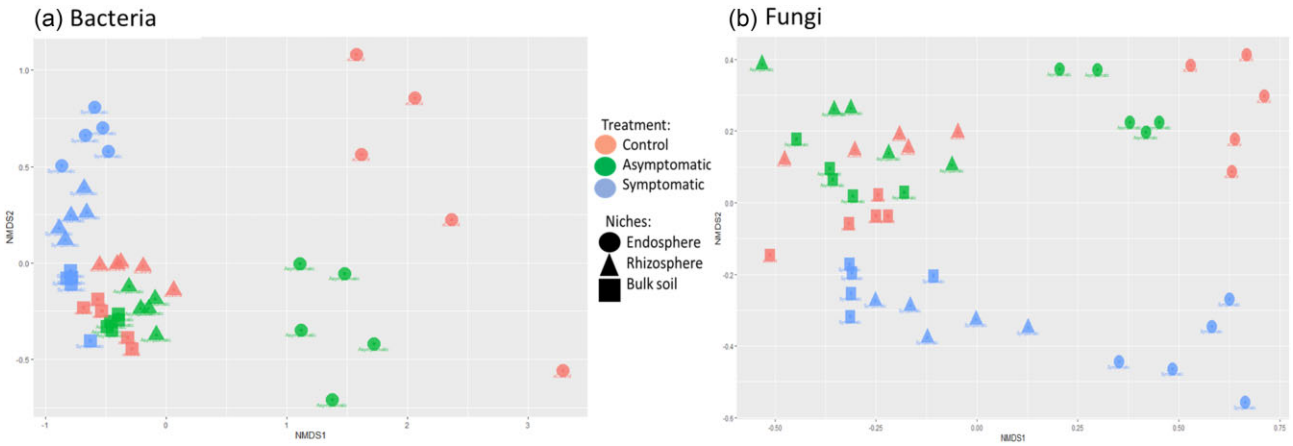

Figure 2. NMDS based on Bray-Curtis dissimilarity index plotted for both prokaryotes and fungi community at all three niches for seedlings of control, asymptomatic, and symptomatic.

asymptomatic samples were compared using Student's *t*-test. All analyses were performed using Microsoft Excel.

Sequence accession numbers

All the raw reads have been deposited at the NCBI. For amplicon sequencing data: bioproject ID PRJNA1110847; biosample accessions from SAMN41387998 to SAMN41388042; and SRA accessions from SRR29229796 to SRR29229840. For nanopore shotgun metagenomics sequencing data: bioproject ID PRJNA798176**,** PRJNA798178, and PRJNA798181; biosample accession SAMN25049936, SAMN25049945, and SAMN25049946; and SRA accessions SRR17966154, SRR17965732, and SRR17966155.

Results

Following 12 months of observation, the *G. boninense* PER 71 inoculated seedlings were categorized according to disease symptoms and assigned a Disease Severity Index (DSI 0–4). Subsequently, 10 control seedlings, 10 treated seedlings with a DSI of 0 (considered asymptomatic), and 10 treated seedlings with a DSI of 4 (deemed symptomatic) were selected for further investigation, following the prescribed methodology.

Microbial community abundance, diversity, and structure

The total read count, richness (Chao 1), and Shannon index for both prokaryotic and fungal communities based on Illumina amplicon sequencing are summarized in Supplementary Table S1, and the significance differences among sample types were summarized in Table 1. Infected seedlings did not lead to any changes in the total read count, richness, or Shannon diversity for both prokaryotic and fungal communities in the bulk soil. Differences in Chao 1 and the Shannon index, but not in total read count, were observed in the prokaryotic community of the rhizosphere when comparing symptomatic and asymptomatic seedlings. However, the fungal community showed no differences between the two groups. Significantly higher read count, richness, and Shannon diversity were observed for the endophytic prokaryotic community in symptomatic seedlings. In contrast to the prokaryotic community, the endophytic fungal community showed lower richness ($P < .05$; Student's *t*-test) and Shannon diversity (although insignificant) in symptomatic seedlings, while no difference in total read count was observed.

As shown in Fig. 2, clear separation of symptomatic samples from control and asymptomatic samples was observed for both prokaryotic (Adonis *P*-value = .001; Permutest.betadisp *P*-value

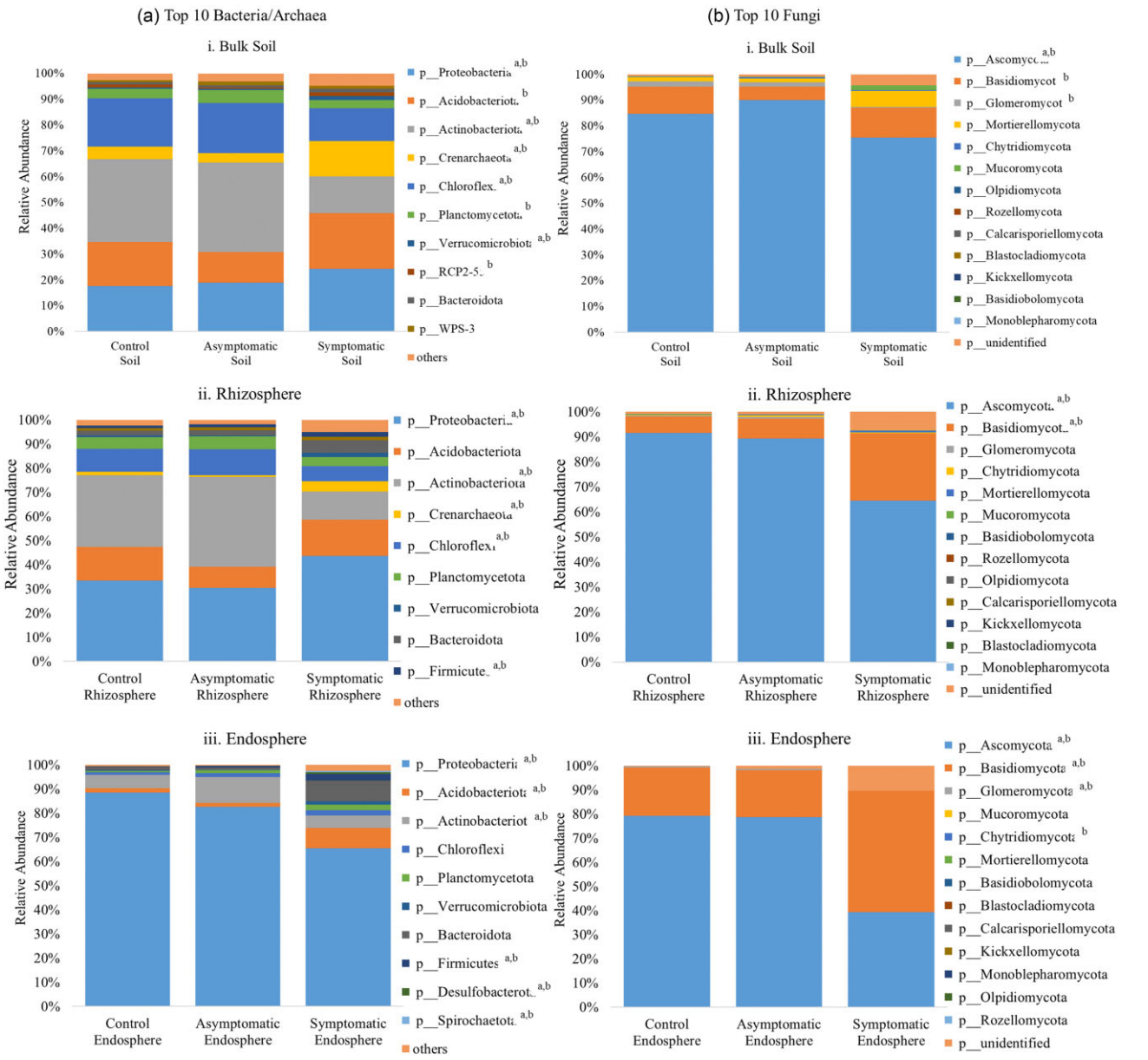

Figure 3. Average relative abundance for prokaryotes (a) and fungi (b) of (i) bulk soil; (ii) rhizosphere; and (iii) endosphere at phylum level in the microbial community for seedlings of control, asymptomatic, and symptomatic. Listed are top 10 most abundant phyla in the community; the "others" in the prokaryotes community referred to sum of phyla with relative abundance <1%. Superscript "a" indicated significant difference in relative abundance between control and symptomatic; "b" indicated significant difference in relative abundance between asymptomatic and symptomatic (Student's *t*-test, $P < .05$, $n = 5$).

> .05) and fungal (Adonis *P*-value = .001; Permutest.betadisp *P*-value > .05) communities, despite the prominent variation driven by niches. When observed at individual niches with particular focus on the asymptomatic seedlings, it was found that asymptomatic samples are separated from control samples as well, except for the prokaryotic community in the rhizosphere (Adonis *P*-value > .05). Details of the R^2 values and *P*-values for Adonis and Permutest.beta-dispersion are provided in Supplementary Table S2.

Taxonomy composition

A total of 2675 584 and 6005 670 sequences were generated from amplicon sequencing for the prokaryotic and fungal communities, respectively, across 45 samples. These sequences were clustered into 4157 OTUs distributed among 37 prokaryotic phyla and 2937 OTUs across 13 fungal phyla. Generally, the prokaryotic OTUs were dominated by the phyla Pseudomonadota (synonym Proteobacteria, 17.6%–88.5%), Acidobacteriota (1.7%–21.6%), Actinobacteriota (5.2%–37.2%), and Chloroflexota (1.1%–19.4%), with their total relative abundance consistently contributing >85% of the total read count across treatments, in the communities of all three niches (Fig. 3ai, ii, and iii). Other dominant (>1% relative abundance) phyla included Bacteroidota, Crenarchaeota, Planctomycetota, and Bacillota, distributed at different ratios across communities of different niches (Fig. 3a; Supplementary Table S3).

Upon exposure to the pathogen, a decrease in relative abundance was observed for the phyla Actinobacteriota and Chloroflexota, while Acidobacteriota consistently showed a drastic increase in relative abundance in all three niches of symptomatic

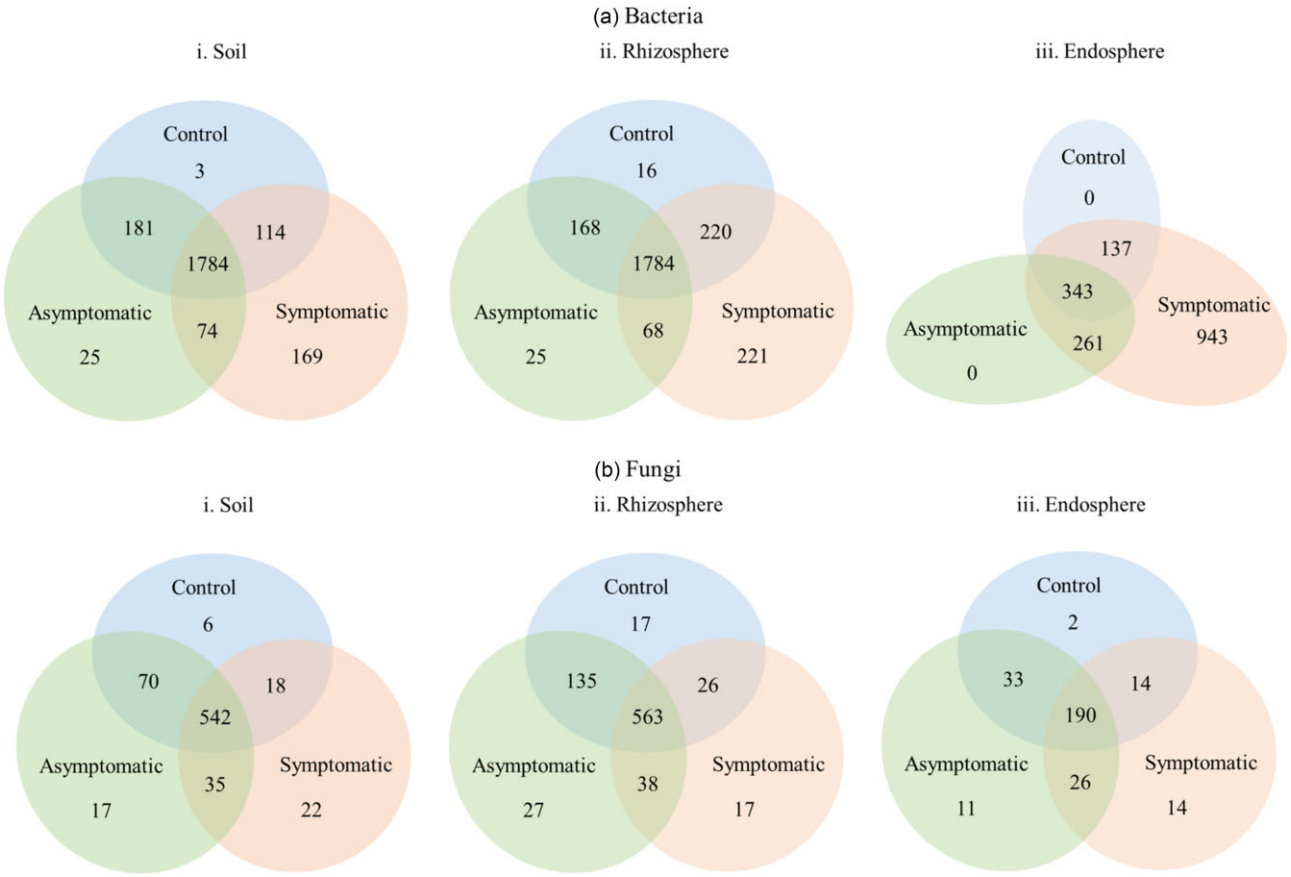

Figure 4. Venn diagram showing the unique and shared OTUs of the (a) prokaryotes and (b) fungal communities for (i) bulk soil; (ii) rhizosphere; and (iii) endosphere across samples of control, asymptomatic, and symptomatic. Only OTUs detected in at least three replicates within group were used in this analysis.

seedlings; this observation was contrary to that for asymptomatic seedlings. The most dominant phyla, Pseudomonadota, showed an increasing trend in relative abundance in both bulk soil and rhizosphere samples from control to asymptomatic to symptomatic samples. However, an opposite trend was observed for Pseudomonadota in the endosphere samples.

The fungal phyla Ascomycota (39.4%–91.5%) and Basidiomycota (5.2%–50.2%) were the most dominant fungi in the community of all samples, accounting for >85% of the total fungal read count. A decrease in the abundance of Ascomycota was associated with pathogen exposure and further decreased in samples with disease symptoms, while an increased abundance of Basidiomycota was associated with disease development (Fig. 3b; Supplementary Table S4).

Shared and unique OTUs in both prokaryotic and fungal communities were identified for all samples (Fig. 4). The highest number of unique prokaryotic OTUs were found in symptomatic samples across all three niches, with a particularly high number in the endosphere samples (Fig. 4a.iii), where the number of unique OTUs exceeded the number of shared OTUs. We observed that >90% of these unique OTUs belonged to rare taxa (<0.1% abundance); only one unique prokaryotic OTU, tentatively identified as *Pseudomonas citronellolis*, was found with a relative abundance of >1% in the endosphere symptomatic sample. The majority of the other abundant unique OTUs (>0.1% relative abundance) associated with symptomatic samples belonged to the phyla Pseudomonadota, Bacteroidota, and Bacillota (Supplementary Table S5). A small number of unique OTUs was observed in asymptomatic bulk soil and rhizosphere, but none were found in the asymptomatic endosphere (Fig. 4a i and ii). All unique OTUs identified in asymptomatic samples had a relative abundance of <0.1% (Supplementary Table S7).

A similar number of unique fungal OTUs were observed in symptomatic and asymptomatic samples. The majority of unique fungal OTUs in both symptomatic and asymptomatic samples were rare taxa with a relative abundance of <0.1%. The unique fungal OTUs with the highest relative abundance belonged to the phylum Basidiomycota in symptomatic bulk soil samples (relative abundance 0.43%) and to the phylum Ascomycota in symptomatic rhizosphere samples (0.85% relative abundance) and symptomatic endosphere samples (0.46% relative abundance) (Supplementary Table S6). All unique OTUs in asymptomatic samples across all three niches had a relative abundance <0.1% (Supplementary Table S8).

We further performed differential analysis using DESeq2 (adjusted *P*-value < .05) to identify OTUs associated with the three groups of seedlings, focusing particularly on OTUs associated with asymptomatic seedlings. Figure 5a and b show the prokaryotic and fungal OTUs that were most significantly enriched in asymptomatic seedlings compared to controls across all three compartments. In bulk soil, prokaryotic OTUs enriched in asymptomatic samples were distributed among the phyla Chloroflexota, Actinobacteriota, and Pseudomonata. In the rhizosphere of asymptomatic seedlings, the most enriched prokaryotic OTUs belonged to the phyla Actinobacteriota, followed by Chloroflexota, Planctomycetota, and Pseudomonata

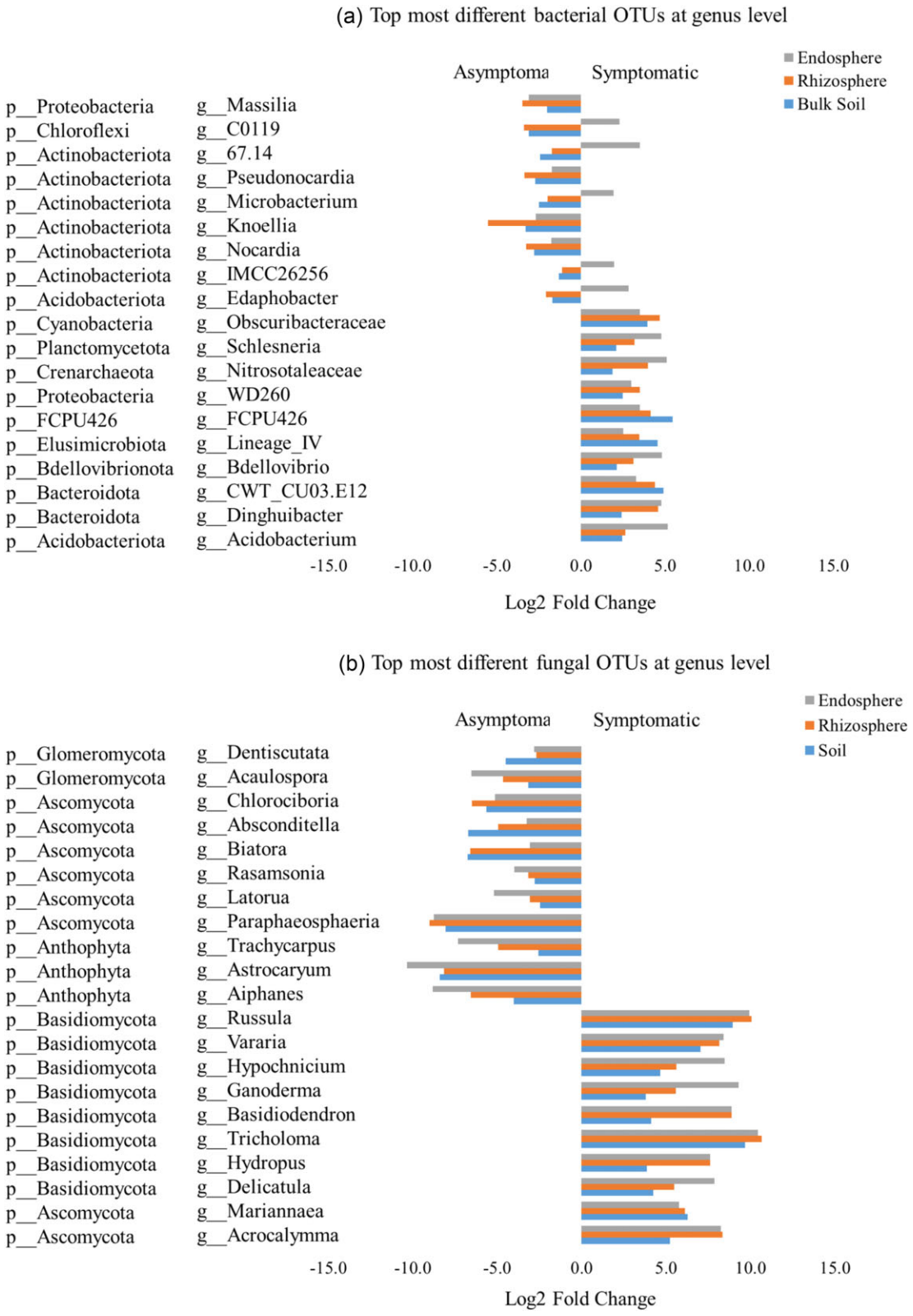

Figure 5. OTUs significantly enriched in seedlings of asymptomatics when compared to control (log2 fold change), for (a) prokaryotes and (b) fungi; listed are OTUs with read counts > 20; *P*-value < .05, $n = 5$. Details of data are provided in Supplementary Tables S12 and S13.

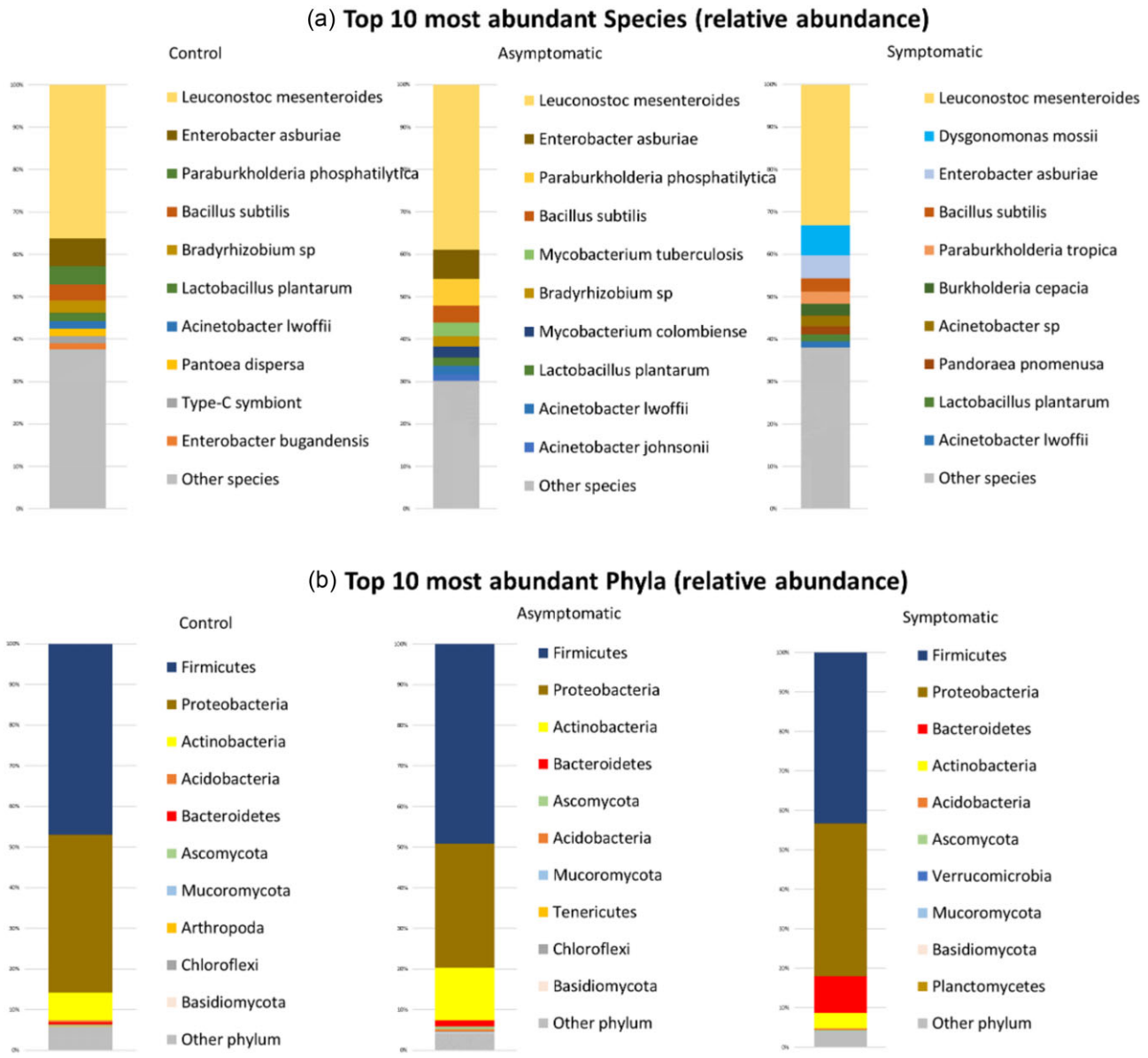

Figure 6. Top 10 most abundant (relative abundance) species (a) and phylum (b) in the rhizosphere for control, asymptomatic, and symptomatic samples based on shotgun metagenomics sequencing by nanopore sequencing technology.

(Supplementary Table S9). Interestingly, no differential OTU was found in the endosphere samples when comparing asymptomatic to control. When comparing asymptomatic to symptomatic samples, the most enriched prokaryotic OTUs belonged to the phyla Actinobacteriota, Bacteroidota, Chloroflexota, and Planctomycetota, with Actinobacteriota and Chloroflexota uniquely enriched in asymptomatic seedlings. Complete information on the differential analysis based on DESeq2 for prokaryotic OTUs is provided in Supplementary Table S11.

The majority of fungal OTUs enriched in asymptomatic seedlings were found to belong to the phylum Ascomycota, followed by the phylum Basidiomycota. This pattern was consistent across the three compartments (Supplementary Table S10). When compared to symptomatic seedlings, only three fungal OTUs were consistently enriched in asymptomatic samples, and they belonged to the phyla Glomeromycota and Ascomycota, with Glomeromycota uniquely enriched in asymptomatic seedlings. OTU 19, annotated as *Ganoderma* sp., was detected in all samples across all niches with varying read counts, as reported in Supplementary Table S6d. In the rhizosphere and endosphere, there was a 6-log2fold and 10-log2fold increase in abundance (Supplementary Table S12, respectively) in symptomatic samples compared to asymptomatic samples. There were no significant differences noticed comparing asymptomatic samples to control for OTU 19. Complete information on the differential analysis based on DESeq2 for fungal OTUs is provided in Supplementary Table S12.

Nanopore sequencing: actinobacteriota as the core defense component

The taxonomic classification of shotgun metagenome reads from rhizosphere samples for control, asymptomatic, and symptomatic seedlings corroborated the results from 16S rRNA gene amplicon sequencing. The 10 most abundant species and phyla are listed in Fig. 6a and b, respectively. Although both asymptomatic and symptomatic samples were artificially inoculated with the

Table 2. Top five most abundant Actinobacteriota in the rhizosphere-asymptomatic sample, number of antimicrobial genes detected, and the respective antimicrobial compound.

Species	Relative abundance (%)			Number of genes detected	Antimicrobial compound
	Control	Asymptomatic	Symptomatic		
Mycobacterium tuberculosis	0.746	3.179	0.151	4	Avermectin, **Bacillomycin D**, Cycloserine, and **Gentamicin A**
M. colombiense	0.538	2.486	0.141	5	Aurachin, Chlortetracycline, Cycloserine, Elloramycin A, and Kanamycin A
M. paraense	0.667	0.964	0.238	4	Aurachin, Avermectin, **Bacilysin**, and Epithienamycin E
Kutzneria buriramensis	0.194	0.621	0.004	17	**Ansamitocin P-3**, Aurachin, Auramycinone, Bacillomycin D, **Bacilysin**, **Cycloserine**, **Gramicidin S**, Kanamycin A, Neocarzinostatin chromophore, **Nocardicin A**, Penicillin N, Pristinamycin IA, **Rhamnolipid**, Rhodomycin, **Syringomycin**, **Tetracycline**, and **Toxoflavin**
M. mantenii	0.13	0.521	0.053	6	Aurachin, Bacillomycin D, **Bacilysin**, Chlortetracycline, Cycloserine, and Kanamycin A

*Antimicrobial compounds in bold are reported with antifungal activities.

Table 3. Top five most abundant Ascomycota in the rhizosphere-asymptomatic sample, number of antimicrobial genes detected, and the respective antimicrobial compound.

Species	Relative abundance (%)			Number of genes detected	Antimicrobial compound
	Control	Asymptomatic	Symptomatic		
Trichoderma asperellum	0.054	0.366	0.144	5	**Bacilysin**, Ditryptophenaline, Cephalosporin C, Rhodomycin, and **Vancomycin**
Penicillium janthinellum	0.012	0.029	0.005	2	**Bacilysin** and Ditryptophenaline
Fusarium oxysporum	0.003	0.023	0.002	7	**Bacilysin**, **Bacillomycin D**, Ditryptophenaline, **Gramicidin S**, Rhodomycin, **Toxoflavin**, and **Vancomycin**
P. oxalicum	0.002	0.02	0.015	2	**Iturin A** and Surfactin
Talaromyces cellulolyticus	0.006	0.019	0.005	3	Ditryptophenaline, Myxalamid S, and **Pentalenolactone**

*Antimicrobial compounds in bold are reported with antifungal activities.

pathogen *G. boninense*, its presence could only be detected in the rhizosphere-symptomatic sample with a relative abundance of 0.00002%.

Upon analyzing the microbial composition, we observed an enrichment of Actinobacteriota in the rhizosphere-asymptomatic sample, including a total of 267 species of Actinobacteriota, of which 180 species are unique to the rhizosphere-asymptomatic sample. More importantly, the population of Actinobacteriota in the rhizosphere-asymptomatic sample is 1.9- and 3.2-fold higher than that in the rhizosphere-control and rhizosphere-symptomatic samples, respectively (Supplementary Table S13). To further investigate the functional correlation between the enrichment of Actinobacteriota and the rhizosphere-asymptomatic sample, we examined the antagonistic properties of Actinobacteriota species by screening the top five most abundant species for antimicrobial synthesis genes, as listed in Table 2. Among the putatively associated antimicrobial compounds, Bacillomycin D, Gentamicin A, Bacilysin, Ansamitocin P-3, Cycloserine, Nocardicin A, Rhamnolipid, Syringomycin, Tetracycline, and Toxoflavin (listed in bold in Table 2) have been reported to possess antifungal activities.

For the fungal communities, the enrichment of Ascomycota and Mucoromycota in the rhizosphere-asymptomatic sample was again observed (Supplementary Table S13). A similar approach was taken where the top five most abundant Ascomycota fungal species in the rhizosphere-asymptomatic sample, as listed in Table 3, were screened for their potential antimicrobial properties. The compounds in bold, as listed in Table 3—Bacilysin, Vancomycin, Bacillomycin D, Ditryptophenaline, Gramicidin S, Toxoflavin, Iturin A, and Pentalenolactone—have been reported to possess antifungal activity.

Co-occurrence networks analysis revealed change of interaction among community members in response to pathogen invasion

We further performed co-occurrence network analysis to better understand the associated changes in microbial interactions. We estimated the topological properties of the whole communities, both prokaryotic and fungal, for all compartments, with particular interest in the features of microbial interactions in the asymptomatic samples compared to the control samples. The

analysis revealed that the prokaryotic community in the bulk soil and rhizosphere of asymptomatic samples is less complex compared to control samples. All the topological properties (nodes, edges, degree, clustering coefficient, betweenness, eigenvector, coreness, eccentricity, diameter, density, and average degree) recorded lower scores, except for coreness, when compared to the control (Fig. 7a; Supplementary Table S14a). In the endosphere samples, an opposite trend was observed, with asymptomatic samples showing increased complexity compared to control samples.

The fungal communities, on the other hand, showed more complex interaction patterns in the asymptomatic samples compared to the control, as indicated by higher scores recorded for most of the topological properties (Fig. 7b; Supplementary Table S14b). Hub analysis was carried out, and 30 putative keystone taxa were identified for the asymptomatic samples of all 3 compartments, based on the highest MCC score, which were further substantiated by other algorithms of the CytoHubba plug-in (Supplementary Table S15a). The majority of estimated putative prokaryotic keystone taxa belonged to the phyla Acidobacteriota, Actinobacteriota, Chloroflexota, and Psedomonadota (Alphaproteobacteria). Most of these putative keystone taxa are rare taxa with a relative abundance of <0.1%, with one or two exceptions, for all compartments (Supplementary Table S15a).

For the estimated putative fungal keystone taxa, the majority belonged to the phylum Ascomycota, with class Dothideomycetes and class Eurotiomycetes being the major classes of origin. When comparing the composition of the 30 estimated keystone taxa among the control, asymptomatic, and symptomatic samples for all three compartments, while a few putative keystones were observed to be overlapping among different sample types for the same compartment, the majority were unique to the sample types (Supplementary Table S15b).

Discussion

Our work is the first to provide detailed descriptions of the whole microbial community, including both prokaryotes and fungi, across bulk soil, rhizosphere, and endosphere of oil palm roots. Furthermore, using full-sibling seedlings under identical environmental conditions is a distinctive approach compared to other studies, reducing variability from genetics, soil, and environment, and leading to more precise interpretations. In this study, we compared the microbial communities with focus on those associated with asymptomatic seedlings, highlighting differences across all three niches. It also serves as a foundation for discovering biomarkers to develop BSR-suppressive soil and resilient planting materials fortified with BSR-suppressing microbes.

Soil prokaryotic diversity has been positively correlated with plant health and biomass (Mazzola 2004, Alami et al. 2020, Chen et al. 2020). In this study, the prokaryotic diversity in the bulk soil was found to be consistent among the control, asymptomatic, and symptomatic samples, despite the infected seedlings showing two outcomes, i.e. asymptomatic and symptomatic. The variations in prokaryotic alpha diversity between asymptomatic and symptomatic seedlings were noticeable in both rhizosphere and endosphere (Supplementary Table S1). This suggests that the response to pathogen invasion is more pronounced closer to the host, rather than in more distant regions like the bulk soil. Increased alpha diversity was reported in infected but symptomless hosts, such as banana tissue culture plantlets (Lian et al. 2008)) and potato plants (Reiter et al. 2002). Similarly, we observed higher prokaryotic richness and diversity in asymptomatic endosphere samples compared to controls. This trend was even more pronounced in fungal communities, where both richness and diversity were elevated across all three niches. This suggests that greater microbial diversity may play a role in defending against pathogen invasion and helping the host remain asymptomatic (Reiter et al. 2002). The exceptional leap, especially in the richness of the fungal communities in the asymptomatic endosphere samples, indicates an unexpected stimulatory in the diversity of the endophytic fungi community when exposed to the pathogen, which could be preventing further disease development. Various mechanisms could be involved, such as out-competing pathogens, producing antibiotics, and triggering systemic resistance (Reiter et al. 2002). However, the highest read count, richness, and Shannon diversity for prokaryotic community were detected in symptomatic endosphere samples (Supplementary Table S1); as indicated by a class 4 DSI, the presence of rotten tissue may explain this phenomenon. A similar observation was reported by Amran et al. (2016), where the prokaryote diversity at the infected zone was higher than non-infected zone. In this study, the high diversity is likely responding to decayed tissue as a source of nutrients and hence proliferation of a rich microbial community.

In both prokaryotic and fungal communities, the main differences in composition were driven by niches, a common pattern in microbial studies (Beckers et al. 2017, Goss-Souza et al. 2020). However, the clear distinction between symptomatic samples and both asymptomatic and control samples in the NMDS plot, indicates noticeable changes in prokaryotic community composition. For the fungal community, a similar clustering pattern was observed but with $< < 0.05$ (F-test) when comparing asymptomatic and symptomatic samples, indicating varying community composition within the group. This could influence the significant results in the Adonis analysis (Supplementary Table S1a), so interpretation should be cautious. Although we expected the fungal and prokaryotic community compositions to be similar between asymptomatic and control samples due to their equally healthy appearance of the hosts, the data revealed significant compositional differences across all niches, particularly in the endosphere communities. This observation aligns with the alpha diversity analysis, where higher richness and diversity were observed in asymptomatic samples, especially in the endosphere. These findings suggest that the microbial community is responding to the pathogen, could be involved in disease progression and influencing the outcome. The endosphere appears to be the most critical site of this microbial interaction. However, we cannot determine the plant-microbe relationship's chronology regarding the battle against pathogen invasion. To address this, a time series experiment combined with multi-omics analysis is necessary to clarify whether the host influences the microbial community by emitting signals or if the microbial community reacts to the pathogen independently, leading to different outcomes.

Several phyla showed significant changes in relative abundance across samples. Actinobacteriota was consistently more abundant in asymptomatic samples compared to the other two groups, at both genus and OTU levels. Actinobacteriota is known for its role in suppressing plant diseases and promoting growth through various mechanisms, such as producing hormones and antibiotics (Palaniyandi et al. 2013). Additionally, genera like *Sphingomonas* spp., *Acidothermus* spp., and *Nocardioides* spp. were also enriched in asymptomatic seedlings and have been associated with disease control (Wachowska et al. 2013, Cipriano et al. 2016, Ou et al. 2019, Legein et al. 2020, Morimura et al. 2020). Shotgun metagenomics sequencing revealed that

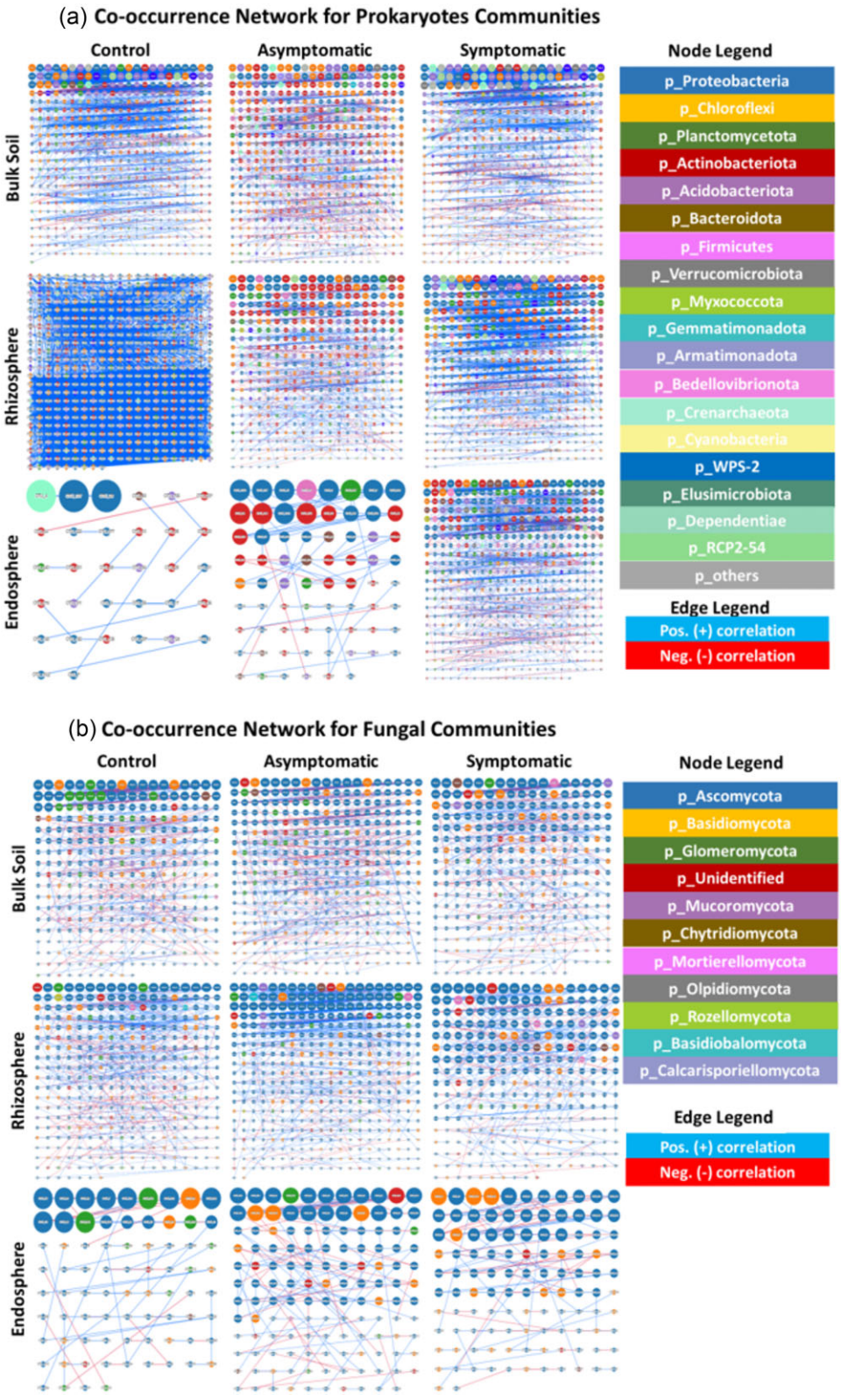

Figure 7. Co-abundance network for microbial communities for (a) prokaryotes community and (b) fungal community; network organized in grid format.

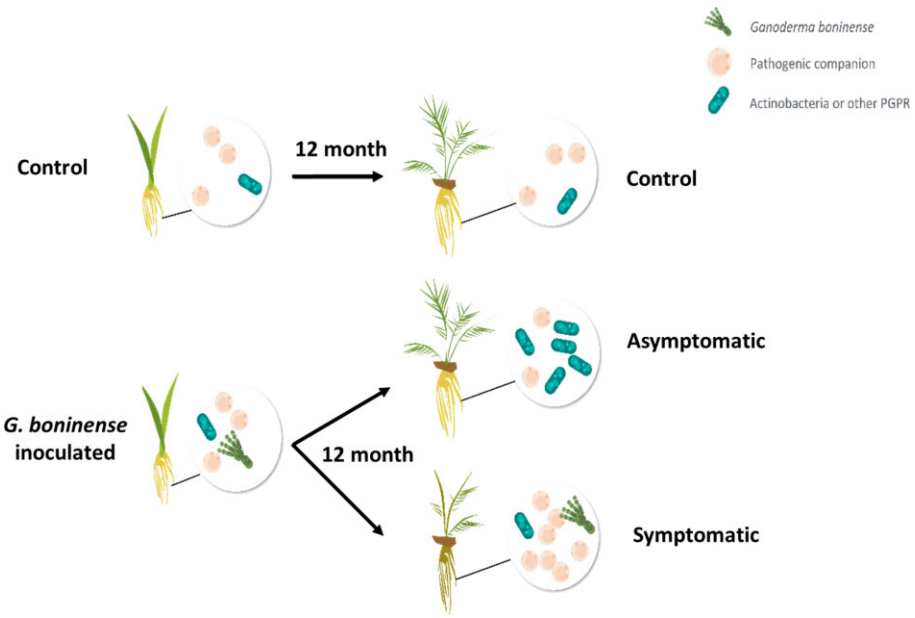

Figure 8. In the asymptomatic seedlings, recruitment of a large and diverse Actinobacteriota community at the root compartments, synthesizes a spectrum of antibiotics and plays a key role in the suppressing *G. boninense* and its related prokaryotes pathogenic companion, thereby protecting the seedling from further invasion of *G. boninense* into the root.

Actinobacteriota in asymptomatic seedlings carry multiple antimicrobial genes, indicating their potential role in defending the host against pathogen invasion. Studies have shown that Actinobacteriota members can antagonize *G. boninense* and are being explored as biocontrol agents in agriculture (Shariffah-Muzaimah et al. 2018, Shariffah-Muzaimah et al. 2020, Sujarit et al. 2020, Budi et al. 2022, Sunaryanto et al. 2023, Rupaedah et al. 2024).

The members of Bacteroidota phylum, *Dysgonomonas mossi*, *Chryseobacterium geocarposphaerae*, and *Bacteroides xylanolyticus* were significantly more abundant in the rhizosphere of symptomatic samples compared to control and asymptomatic samples. It is worth noting that *Dysgonomonas mossi* and *Bacteroides xylanolyticus* are known for their high xylan-degrading enzyme activity (Mirande et al. 2010, Mardina et al. 2016), while *Chryseobacterium* sp. can break down lignin (Tan et al. 2018). As the disease progressed, the decaying roots of symptomatic seedlings became a rich food source for these bacteria. The fungal phyla Glomeromycota was remarkably enriched in asymptomatic samples across all three niches; Glomeromycota are known for promoting plant growth by forming symbiotic relationships with ~80% of land plants, where their fungal hyphae enter plant roots and exchange nutrients (Taylor et al. 2015). Additionally, two OTUs belonging to class Dothideomycetes and class Leotiomycetes of the Ascomycota were consistently enriched in asymptomatic samples; both are known to have biocontrol capabilities (Thambugala et al. 2020).

The *Trichoderma* spp., which are widely used as fungal biocontrol agents in various crops (Kumar and Ashraf 2017), including against BSR in oil palm (Sundram et al. 2008), was examined too. We found two *Trichoderma* OTUs: *T. asperellum* and *T. virens*. Interestingly, *T. asperellum* was associated with asymptomatic samples, while *T. virens* was associated with symptomatic samples, although neither was significantly enriched in their respective samples. However, when we used shotgun metagenomics sequencing, we discovered that *T. asperellum* was the most abundant species in the rhizosphere of asymptomatic samples, showing a significant increase compared to control and symptomatic samples (Supplementary Table S16). Several studies have also used *T. asperellum* as a biological control agent against *G. boninense* (Jawak et al. 2018, Musa et al. 2018, Muniroh et al. 2019).

OTU 19, identified as *Ganoderma* sp., showed a 6-log2fold and 10-log2fold increase in abundance in the symptomatic samples in the rhizosphere and endosphere compared to asymptomatic samples, respectively. The detection of significant read counts (>100) in the bulk soil and rhizosphere of asymptomatic samples confirmed the presence of pathogen inoculum in the polybag, indicating that the seedlings' asymptomatic condition was not due to pathogen avoidance. This also implies that the manifestation of disease is linked to the composition and function of the microbial community, not just the abundance of the pathogen (Xiong et al. 2017).

Network analysis uncovered subtle changes in microbial interaction patterns indicated by network topological properties (Supplementary Table S13). For instance, in the bulk soil prokaryotes community, asymptomatic samples showed a lower number of nodes, edges, and degrees, but notably higher betweenness (0.25) compared to control (0.02), suggesting more efficient information flow across the network. Similar trend was observed for rhizosphere and endosphere samples for the prokaryote communities. It was noticed that there was a higher percentage of negative interaction in the asymptomatic—bulk soil and rhizosphere prokaryotes community compared to control. A higher number of negative interactions suggests a greater degree of competition (Ou et al. 2019) within the network, which indicates a more complex interaction along with pathogen invasion in the asymptomatic seedling.

Keystone taxa are crucial species whose removal could disrupt a community (Wu et al. 2023). Our analysis identified distinct groups of potential keystone taxa across three compartments, with limited overlap among samples. Once again, several members of Actinobacteriota emerged as potential keystone taxa for asymptomatic samples. Interestingly, Actinobacteriota were prominent at the top of the network grid, indicating their importance compared to control and symptomatic samples across all

three compartments (Fig. 7). Most of the estimated keystone taxa in our study belonged to rare taxa with a relative abundance of <0.1%. It is common to find rare species as keystones, as their abundance does not necessarily dictate their importance (Lynch and Neufeld 2015, Jousset et al. 2017, Banerjee et al. 2018, Banerjee et al. 2019). In addition, several studies highlight the significance of rare taxa in geo-cycling processes like nitrogen, sulfur, and carbon cycling (Jousset et al. 2017, Jia et al. 2018); disruption of these cycles could harm ecosystems. These findings underscore the potential importance of rare species as keystone species.

Conclusion

Our findings reveal significant shifts in microbial communities in oil palm seedlings in response to pathogen invasion, with distinct responses observed across different niches, particularly the endosphere. We noted that resident microbial communities can exhibit varied responses to pathogen challenge, and that members of the same phylum may have different roles in host–microbe interactions.

We also observed the recruitment of beneficial microbes in asymptomatic seedlings, notably members of the Actinobacteriota and Ascomycota phyla. The consistent association of these taxa with asymptomatic seedlings suggests their importance in host defense mechanisms. We hypothesize that the diversity within Actinobacteriota and Ascomycota communities may contribute to the production of a range of antibiotics, thereby suppressing *G. boninense* and associated pathogenic Bacteroidota, providing protection to the saplings (Fig. 8). This study is the first to indicate the potential role of Actinobacteriota and Ascomycota in controlling BSR disease.

However, the factors driving these community shifts and the intricacies of microbe–pathogen–host interactions remain to be fully understood. Comprehensive profiling using shotgun metagenome sequencing or metatranscriptomics in a time series experiment could offer deeper insights, potentially guiding the development of more resilient oil palm varieties. Additionally, isolating and screening cultivable strains from these experiments may yield microbial cultures with direct defensive roles, paving the way for the creation of synthetic microbial communities for practical applications in agriculture.

Acknowledgments

We thank Dr Neoh Bee Keat, Dr Nalisha Itnin, Agronomic Selection Unit, Biotech and Breeding, SD Guthrie Technology Centre Sdn. Bhd., for their generous help of sample preparation and collection. Ms Joyce Ding Yoon Mei, Industrial Microbiology, Biotech, and Breeding, SD Guthrie Technology Centre Sdn. Bhd., for her assistance in graph constructions.

Author contributions

Lisim Ho (Conceptualization, Data curation, Formal analysis, Investigation, Methodology, Validation, Visualization, Writing – original draft), Chengyu Lai (Data curation, Formal analysis, Software, Validation), Leona D.J. Daim (Conceptualization, Methodology, Validation), Normahnani M. Noh (Conceptualization, Data curation, Methodology), Yunci Yap (Data curation, Methodology), Julia Ibrahim (Project administration, Resources, Supervision, Writing – review & editing), and Cheekeng Teh (Conceptualization, Funding acquisition, Resources, Supervision, Validation, Writing – review & editing)

Supplementary data

Supplementary data is available at FEMSEC *Journal* online.

Conflict of interest: None declared.

Funding

This work was supported by SD Guthrie Research Sdn Bhd, Malaysia.

References

Ahmadi P, Muharam FM, Ahmad K *et al.* Early detection of *Ganoderma* basal stem rot of oil palms using artificial neural network spectral analysis. *Plant Dis* 2017;**101**:1009–16.

Alami MM, Xue J, Ma Y *et al.* Structure, diversity, and composition of bacterial communities in rhizospheric soil of coptis chinensis franch under continuously cropped fields. *Diversity* 2020;**12**:57.

Amran A, Jangi MS, Aqma WS *et al. Bacterial Diversity of Oil Palm Elaeis guineensis Basal Stems*, Vol. **1784**. Melville (NY): AIP Publishing LLC, 2016, 020024.

Anothai J, Chairin T. Analysis of rhizobacterial community associated with the occurrence of *Ganoderma* basal stem rot disease in oil palm by Illumina next-generation sequencing. *Arch Microbiol* 2022;**204**:1–10.

Banerjee S, Schlaeppi K, van der Heijden MG. Keystone taxa as drivers of microbiome structure and functioning. *Nat Rev Microbiol* 2018;**16**:567–76.

Banerjee S, Walder F, Büchi L *et al.* Agricultural intensification reduces microbial network complexity and the abundance of keystone taxa in roots. *ISME J* 2019;**13**:1722–36.

Beckers B, De Beeck MO, Weyens N *et al.* Structural variability and niche differentiation in the rhizosphere and endosphere bacterial microbiome of field-grown poplar trees. *Microbiome* 2017;**5**:25.

Budi MBS, GIYANTO G, Tondok ET. Isolation of actinomycetes from peatland to suppress the growth of *Ganoderma boninense* the causal agent of basal stem rot disease in oil palm. *Biodivers J Biol Divers* 2022;**23**:5914.

Chin C-H, Chen S-H, Wu H-H *et al.* cytoHubba: identifying hub objects and sub-networks from complex interactome. *BMC Syst Biol* 2014;**8**:1–7.

Chen Q-L, Ding J, Zhu Y-G *et al.* Soil bacterial taxonomic diversity is critical to maintaining the plant productivity. *Environ Int* 2020;**140**:105766.

Chong KP, Dayou J, Alexander A. Detection and control of *Ganoderma boninensein* oil palm crop. *Springer Briefs Agric* 2017;**20**:20.

Chong KP, Ho CM, Dayou J *et al.* Preliminary observation of phenolic acids on basal stem rot infected oil palm. *The Planter* 2020;**96**:379–86.

Cipriano MAP, Lupatini M, Lopes-Santos L *et al.* Lettuce and rhizosphere microbiome responses to growth promoting *Pseudomonas* species under field conditions. *FEMS Microbiol Ecol* 2016;**92**:fiw197.

Durand-Gasselin T, Asmady H, Flori A *et al.* Possible sources of genetic resistance in oil palm (*Elaeis guineensis* Jacq.) to basal stem rot caused by *Ganoderma boninense*—prospects for future breeding. *Mycopathologia* 2005;**159**:93–100.

Flood J. A review of *Fusarium* wilt of oil palm caused by *Fusarium oxysporum* F. sp. *elaeidis*. *Phytopathology* 2006;**96**:660–2.

Goh YK, Marzuki NF, Tuan Pa TNF *et al.* Biocontrol and plant-growth-promoting traits of *Talaromyces apiculatus* and *Clonostachys rosea* consortium against *Ganoderma* basal stem rot disease of oil palm. *Microorganisms* 2020;**8**:1138.

Gorea E, Godwin I, Mudge A. *Ganoderma* infection of oil palm—a persistent problem in Papua New Guinea and Solomon Islands. *Austra Plant Pathol* 2020;**49**:1–9.

Goss-Souza D, Mendes LW, Rodrigues JLM *et al.* Ecological processes shaping bulk soil and rhizosphere microbiome assembly in a long-term Amazon forest-to-agriculture conversion. *Microb Ecol* 2020;**79**:110–22.

Husin NA, Khairunniza-Bejo S, Abdullah AF *et al.* Application of ground-based LiDAR for analysing oil palm canopy properties on the occurrence of basal stem rot (BSR) disease. *Sci Rep* 2020;**10**: 1–16.

Iasmartua S. Endophytes identification in healthy and *Ganoderma boninense* infected oil palm using next generation sequencing. Jakarta: Indonesia International Institute for Life Sciences, 2018.

Ibrahim MS, Seman IA, Rusli MH *et al.* Surveillance of *Ganoderma* disease in oil palm planted by participants of the smallholders replanting incentive scheme in Malaysia. *J Oil Palm Res* 2020;**32**: 237–44.

Jackson G. *Pacific Pests and Pathogens—Fact Sheets*. Canberra ACT: Australian Centre for International Agricultural Research, 2017.

Jawak G, Widajati E, Palupi ER *et al.* Oil palm seed coating with enriched *Trichoderma asperellum* (T13) to suppress infection of *Ganoderma boninense* pat. *J Perbenihan Tanaman Hutan* 2018;**6**:121–32.

Jia X, Dini-Andreote F, Salles JF. Community assembly processes of the microbial rare biosphere. *Trends Microbiol* 2018;**26**:738–47.

Jochum MD, McWilliams KL, Pierson EA *et al.* Host-mediated microbiome engineering (HMME) of drought tolerance in the wheat rhizosphere. *PLoS One* 2019;**14**:e0225933.

Jones P, Garcia BJ, Furches A *et al.* Plant host-associated mechanisms for microbial selection. *Front Plant Sci* 2019;**10**:862.

Jousset A, Bienhold C, Chatzinotas A *et al.* Where less may be more: how the rare biosphere pulls ecosystems strings. *ISME J* 2017;**11**:853–62.

Khaled AY, Abd Aziz S, Bejo SK *et al.* A comparative study on dimensionality reduction of dielectric spectral data for the classification of basal stem rot (BSR) disease in oil palm. *Comput Electron Agric* 2020;**170**:105288.

Khosrokhani M, Khairunniza-Bejo S, Pradhan B. Geospatial technologies for detection and monitoring of *Ganoderma* basal stem rot infection in oil palm plantations: a review on sensors and techniques. *Geocarto Int* 2018;**33**:260–76.

Kresnawaty I, Mulyatni A, Eris D *et al.* Electronic nose for early detection of basal stem rot caused by *Ganoderma* in oil palm. *Earth Environ Sci* 2020;**468**:012029.

Kumar M, Ashraf S. Role of *Trichoderma* spp. as a biocontrol agent of fungal plant pathogens. In: *Probiotics and Plant Health*. New York, NY: Springer, 2017, 497–506.

Legein M, Smets W, Vandenheuvel D *et al.* Modes of action of microbial biocontrol in the phyllosphere. *Front Microbiol* 2020;**11**:1619.

Lian J, Wang Z, Zhou S. Response of endophytic bacterial communities in banana tissue culture plantlets to *Fusarium* wilt pathogen infection. *J Gen Appl Microbiol*. 2008;**54**: 83–92.

Lo RKS, Chong KP. Metagenomic data of soil microbial community in relation to basal stem rot disease. *Data in Brief* 2020;**31**:106030.

Lynch MD, Neufeld JD. Ecology and exploration of the rare biosphere. *Nat Rev Microbiol* 2015;**13**:217–29.

Maluin FN, Hussein MZ, Yusof NA *et al.* A potent antifungal agent for basal stem rot disease treatment in oil palms based on chitosan-dazomet nanoparticles. *Int J Mol Sci* 2019;**20**:2247.

Mardina P, Li J, Patel SK *et al.* Potential of immobilized whole-cell *Methylocella tundrae* as a biocatalyst for methanol production from methane. *J Microbiol Biotechnol* 2016;**26**:1234–41.

Mazzola M. Assessment and management of soil microbial community structure for disease suppression. *Annu Rev Phytopathol* 2004;**42**:35–59.

Mendes R, Kruijt M, De Bruijn I *et al.* Deciphering the rhizosphere microbiome for disease-suppressive bacteria. *Science* 2011;**332**:1097–100.

Mirande C, Kadlecikova E, Matulova M *et al.* Dietary fibre degradation and fermentation by two xylanolytic bacteria *Bacteroides xylanisolvens* XB1AT and *Roseburia intestinalis* XB6B4 from the human intestine. *J Appl Microbiol* 2010;**109**:451–60.

Morimura H, Ito M, Yoshida S *et al.* *In vitro* assessment of biocontrol effects on *Fusarium* head blight and deoxynivalenol (DON) accumulation by DON-degrading bacteria. *Toxins* 2020;**12**:399.

Muniroh M, Nusaibah S, Vadamalai G *et al.* Proficiency of biocontrol agents as plant growth promoters and hydrolytic enzyme producers in *Ganoderma boninense* infected oil palm seedlings. *Curr Plant Biol* 2019;**20**:100116.

Musa H, Nusaibah S, Khairulmazmi A. Assessment on *Trichoderma* spp. mixture as a potential biocontrol agent of *Ganoderma boninense* infected oil palm seedlings. *J Oil Palm Res* 2018;**30**:403–15.

Nomanbhay S, Salman B, Hussain R *et al.* Microwave pyrolysis of lignocellulosic biomass—a contribution to power Africa. *Energy Sustain Soc* 2017;**7**:23.

Normahnani Mohd Noh CSSaSA. Screening for *Ganoderma* disease tolerant oil palm progenies in Sime Darby. 2016.

Ou Y, Penton CR, Geisen S *et al.* Deciphering underlying drivers of disease suppressiveness against pathogenic *Fusarium oxysporum*. *Front Microbiol* 2019;**10**: 2535.

Palaniyandi SA, Yang SH, Zhang L *et al.* Effects of actinobacteria on plant disease suppression and growth promotion. *Appl Microbiol Biotechnol* 2013;**97**:9621–36.

Parada AE, Needham DM, Fuhrman JA. Every base matters: assessing small subunit rRNA primers for marine microbiomes with mock communities, time series and global field samples. *Environ Microbiol* 2016;**18**:1403–14.

Pilotti CA, Sanderson FR, Aitken EA. Sexuality and interactions of monokaryotic and dikaryotic mycelia of *Ganoderma boninense*. *Mycol Res* 2002;**106**:1315–22.

Rees R, Flood J, Hasan Y *et al.* Effects of inoculum potential, shading and soil temperature on root infection of oil palm seedlings by the basal stem rot pathogen *Ganoderma boninense*. *Plant Pathol* 2007;**56**:862–70.

Rees R, Flood J, Hasan Y *et al.* Basal stem rot of oil palm (*Elaeis guineensis*); mode of root infection and lower stem invasion by *Ganoderma boninense*. *Plant Pathol* 2009;**58**:982–9.

Reiter B, Pfeifer U, Schwab H *et al.* Response of endophytic bacterial communities in potato plants to infection with *Erwinia carotovora* subsp. *atroseptica*. *Appl Environ Microbiol* 2002;**68**:2261–8.

Rupaedah B, Prasetyo AE, Hidayat F *et al.* Evaluation of microbial biocontrol agents for *Ganoderma boninense* management in oil palm nurseries. *J Saudi Soc Agric Sci* 2024;**23**:236–44.

Shariffah-Muzaimah S, Idris A, Madihah A *et al.* Characterization of *Streptomyces* spp. isolated from the rhizosphere of oil palm and evaluation of their ability to suppress basal stem rot disease in oil palm seedlings when applied as powder formulations in a glasshouse trial. *World J Microbiol Biotechnol* 2018;**34**:1–14.

Shariffah-Muzaimah SA, Idris AS, Nur-Rashyeda R *et al.* Impact of pre-inoculating soil with *Streptomyces* sp. GanoSA1 on oil palm growth and *Ganoderma* disease development. *Biocatal Agric Biotechnol* 2020;**29**:101814.

Subagio A, Foster H. Implications of *Ganoderma* disease on loss in stand and yield production of oil palm in North Sumatra. Kuala Lumpur: Proceedings of the MAPPS Conference (Aug 2003), 2003.

Sujarit K, Pathom-aree W, Mori M *et al.* *Streptomyces palmae* CMU-AB204T, an antifungal producing-actinomycete, as a potential biocontrol agent to protect palm oil producing trees from basal stem rot disease fungus, *Ganoderma boninense*. *Biol Control* 2020;**148**:104307.

Sulaiman S, Othman NQ, Tan JS *et al.* Draft genome assembly dataset of the basidiomycete pathogenic fungus, *Ganoderma boninense*. *Data in Brief* 2020;**29**:105167.

Sunaryanto R, Lentaya HO, Putra I *et al.* *Streptomyces costaricanus* RS25 with bioactivity against plant pathogenic fungus, Vol. **2972**. Melville, NY: AIP Publishing, 2023.

Sundram S, Abdullah F, Ahmad ZAM *et al.* Efficacy of single and mixed treatments of *Trichoderma harzianum* as biocontrol agents of *Ganoderma* basal stem rot in oil palm. *J Oil Palm Res* 2008;**20**: 470–83.

Tan H, Miao R, Liu T *et al.* A bifunctional cellulase–xylanase of a new chryseobacterium strain isolated from the dung of a straw-fed cattle. *Microb Biotechnol* 2018;**11**:381–98.

Taylor TN, Krings M, Taylor EL. 7–Glomeromycota. In: Taylor TN, Krings M, Taylor EL (eds), *Fossil Fungi*. San Diego: Academic Press, 2015, 103–28.

Thambugala KM, Daranagama DA, Phillips AJ *et al.* Fungi vs. fungi in biocontrol: an overview of fungal antagonists applied against fungal plant pathogens. *Front Cell Infect Microbiol* 2020;**10**: 604923.

Turnbull N, de Franqueville H, Breton F *et al.* Breeding methodology to select oil palm planting material partially resistant to *Ganoderma boninense*. In: *5th quadrennial International Oil Palm Conference*. Bali: Bali Nusa Dua Convention Center, 2014, 17–9.

Turner PD. *Oil Palm Diseases and Disorders*. Oxford: Oxford University Press, 1981.

Virdiana I, Rahmaningsih M, Forster BP *et al.* *Trichoderma: Ganoderma Disease Control in Oil Palm: A Manual*. Oxfordshire: CABI, 2019.

Wachowska U, Irzykowski W, Jędryczka M *et al.* Biological control of winter wheat pathogens with the use of antagonistic Sphingomonas bacteria under greenhouse conditions. *Biocontrol Sci Technol* 2013;**23**:1110–22.

White T. Amplification and direct sequencing of fungal ribosomal RNA genes for phylogenetics. In: *PCR Protocols, A Guide to Methods and Applications*. San Diego (CA): Academic Press, Inc, 1990.

Woittiez LS, van Wijk MT, Slingerland M *et al.* Yield gaps in oil palm: a quantitative review of contributing factors. *Eur J Agron* 2017;**83**:57–77.

Wong MY, Govender NT, Ong CS. RNA-seq data of *Ganoderma boninense* at axenic culture condition and under in planta pathogen-oil palm (*Elaeis guineensis* Jacq.) interaction. *BMC Res Notes* 2019;**12**:1–3.

Wu C, Yan B, Wei F *et al.* Long-term application of nitrogen and phosphorus fertilizers changes the process of community construction by affecting keystone species of crop rhizosphere microorganisms. *Sci Total Environ* 2023;**897**:165239.

Xiong W, Li R, Ren Y *et al.* Distinct roles for soil fungal and bacterial communities associated with the suppression of vanilla *Fusarium* wilt disease. *Soil Biol Biochem* 2017;**107**:198–207.

Received 2 August 2024; **revised** 5 September 2024; **accepted** 11 September 2024